FULL PAPER

Dalton
www.rsc.org/dalton

Olefin insertion in the Ru–H and Ru–F bonds of pentacoordinated d^6 Ru(II) species: a DFT study

Hélène Gérard † and Odile Eisenstein *

Laboratoire de Structure et Dynamique des Systèmes Moléculaires et Solides (UMR 5636), Université Montpellier 2, 34095 Montpellier Cedex 05, France.
E-mail: odile.eisenstein@univ-montp2.fr

Received 10th October 2002, Accepted 20th December 2002
First published as an Advance Article on the web 3rd February 2003

DFT (B3PW91) calculations have been carried out to study the impact of a spectator ligand X on the insertion of ethylene into the Ru–H bond of RuL_2HX^{+q} (X = Cl, q = 0, X = CO, q = 1, L = PH_3). It is shown that the energy barrier is higher for X = CO than Cl, which is related to the energy to distort RuL_2HX^{+q} on going from the ground state to transition state. The insertion of fluoroethylene into the Ru–H bond of RuL_2HCl shows that the fluorine substituent on the olefine does not influence much the energy of the reaction, and that insertion yields preferably an α-F substituted ethyl complex. Insertion of ethylene into the Ru–F bond of RuL_2FCl has also been studied. It is found to have a higher activation barrier compared to the insertion of ethylene in the Ru–H bond.

Introduction

Insertion of a coordinated olefin in a metal-H bond and its reverse reaction, β-H abstraction (Scheme 1) play an important role in organometallic chemistry.[1] For example, these steps control the chain length and branching in olefin polymerization. They also control alkane dehydrogenation and olefin isomerization reactions. Hydrogen migration within an alkyl ligand can be achieved using these two elementary processes. These reactions have been extensively studied by theoretical methods either individually or as part of multi-step reactions.[2,3] Whereas various metal fragments have been considered, systematic studies that address the influence of ligands and substituents that are either strong π-donor or π-accceptor are rare.[3]

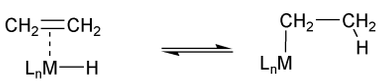

Scheme 1

In this study, we explore the consequences of changing the ligands at the metal center and the substituents on the olefin. The convenient experimental system RuL_2HX^{+q} (X = Cl, q = 0, X = CO, q = 1, L = trialkylphosphine) was chosen since the tetracoordinate 14-electron (d^6) complexes react with unsaturated alkynes and alkenes to give products which depend on the nature of X and of the organic ligand.[4–6] Theoretical studies in the case of acetylene and ethylene (X = Cl, L = PH_3) have shown that the insertion reaction and β-abstraction are key reactive features of these chemical systems.[4,5] In what way would these steps be influenced by the change of X from a π-donor ligand, like Cl^-, to a π-acceptor group, such as CO, or by the replacement of ethylene by fluoroethylene? These important changes can modify significantly the electronic properties of the reactants and thus the energy pattern of these representative elementary reactions.

Computational details

DFT (B3PW91) calculations[7,8] have been carried out using the GAUSSIAN 98 (version A.7) set of programs.[9] Geometry optimization has been carried out without symmetry constraints using the default algorithm. The Hay–Wadt relativistic pseudo-potentials[10] have been used to represent the 28 innermost core electrons of Ru and the 10 core electrons of P and Cl with the associated basis sets[11] for the valence shell. Polarization d functions have been added for Cl and P.[12] The 6-31G** basis set has been used for H, C, O and F.[13] The nature of the extrema (transition state or minimum) has been checked through analytical computation of the Hessian matrix. The harmonic frequencies have been used to calculate the ZPE, the thermal and entropic effects. In most cases, they have no influence. For this reason, these corrections are presented only when significant. A slight perturbation of the geometry of the saddle point associated with a geometry optimization has allowed connecting each transition state to the associated minima.

Results and discussion

(1) RuL_2ClH and $RuL_2(CO)H^+$ (L = PH_3) with ethylene

The local minima are ethylene and β-agostic ethyl complexes that are numbered **1**–**4**; the associated transition states are numbered **5** and **6**. The main geometrical features of these extrema are presented in Fig. 1. The energies are given relative to the ethylene complexes. Coordination of ethylene to $RuL_2(Cl)H$ or $RuL_2(CO)H^+$, which are both electron deficient species (14-electron), occurs prior to insertion into the Ru–H bond. The relative orientation and site of coordination of ethylene to these metal fragments have been discussed previously.[14] In this work, the reactant is considered to be the isomer that is connected to the TS of insertion even when this isomer is only a local minimum. The ethylene ligand is thus always *cis* to the hydride and parallel to the Ru–H bond.

The 16-electron ethylene complexes **1** (X = Cl, q = 0) and **3** (X = CO, q = 1) are square-based pyramids with apical H. Because of the π-donor effect of Cl, the C–C bond is longer and the Ru–C bonds are shorter for X = Cl than for X = CO. This is associated with a larger bond dissociation energy (BDE) of ethylene in **1** (39.2 kcal mol^{-1}) than in **3** (28.8 kcal mol^{-1}). These values correspond to fully optimized complexes and separated fragments. The alkyl complexes **2** (X = Cl, q = 0) and **4** (X = CO, q = 1) are four-coordinate 14-electron complexes. The preferred geometry for this coordination number and electron count has been shown to be an octahedron with two missing *cis* ligands.[4] Therefore the ethyl group can establish a β-agostic interaction at one of the empty coordination sites.[5,15] The geometrical features of these ethyl complexes have been presented in detail.[5,14] The agostic C_2–H bond is considerably longer in **2** (X = Cl, 1.221 Å) than in **4** (X = CO, 1.150 Å). A narrower

† Present address: Laboratoire de Chimie Théorique (UMR 7616), tours 22–23 Université Pierre et Marie Curie, 4 Place Jussieu 75252 Paris Cedex 5 France.

DOI: 10.1039/b209951a

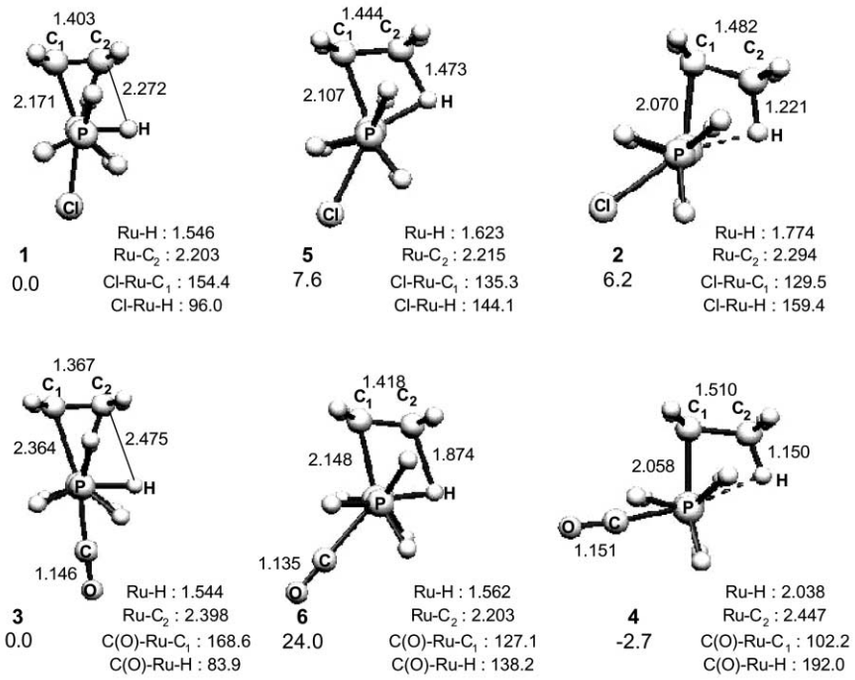

Fig. 1 Structures and relative energies of minima and transition states for the insertion of ethylene in the Ru–H bond for $RuL_2HX(C_2H_4)^{+q}$: X = Cl, $q = 0$ (top) and CO, $q = 1$ (bottom). Distances are in Å, angles in °, energies in kcal mol^{-1}. The energy references are the ethylene complexes.

$Ru–C_1–C_2$ angle is associated with the more elongated C_2–H bond. These features are clear evidence for a stronger agostic interaction in the case of Cl. Insertion of ethylene in the Ru–H bond is only energetically favorable for X = CO, (**3** is 2.7 kcal mol^{-1} above the ethyl complex **4**). In contrast, the insertion is unfavorable for X = Cl since the ethylene complex, **1**, is 6.2 kcal mol^{-1} below the ethyl complex, **2**. The stronger agostic interaction in the later is inconsistent with this energy pattern. It was previously shown that the unfavorable energy of reaction for X = Cl is due to the stronger BDE of ethylene in the reactant.[14]

In the transition states (TS) **5** (X = Cl, i 718.8 cm^{-1}) and **6** (X = CO, i 588.1 cm^{-1}), the CH_2–CH_2 ··· H moiety has geometrical features closer to that in the hydrido–ethylene complex than in the alkyl complex (Fig. 1). The Ru ··· H distances are short (1.623 Å, X = Cl; 1.563 Å, X = CO) and the C–H distances much longer than a normal C–H bond (1.473 and 1.874 Å, respectively, relative to 1.09 Å in alkanes). These transition states differ mostly from the hydrido–ethylene complex by the value of the X–Ru–H angle. The X–Ru–H angle is significantly wider at the TS (144.1° in **5** and 138.2° in **6**) than in the ethylene complexes (96.0° in **1** and 83.9° in **3**).

Since the reaction is endothermic for X = Cl, the Hammond postulate predicts that the TS has a slightly more pronounced ethyl character in the case of Cl.[16] This is apparent in the differences of the Ru–H and C–H distances in transition states **5** and **6**. In the case of Cl, the Ru–H distance is longer and the C–H distance shorter than for CO. All other geometrical features of the TS are similar when changing Cl into CO. It is thus not possible to apply the Hammond postulate to all geometrical variables. For instance, for X = CO, the Ru ··· C_2 varies in a non-monotonous manner from reactant to product. It is shorter in the TS **6** (2.204 Å) than in the olefin complex **3** (2.399 Å) and the alkyl product **4** (2.447 Å). For X = Cl (**5**) the Ru ··· C_2 distance remains almost constant from the reactant **1** to the TS **5** (2.203 to 2.215 Å), and is significantly longer in the product **2** (2.294 Å).

The energy barrier to reach the transition states from the ethylene complexes is significantly higher for X = CO than for X = Cl. The TS **5** (X = Cl) is only 7.7 kcal mol^{-1} above the ethylene complex **1**, *i.e.* 1.5 kcal mol^{-1} above the alkyl product **2**. In contrast, TS **6** (X = CO) is 23.8 kcal mol^{-1} above **3**, *i.e.* more than 25 kcal mol^{-1} above the alkyl complex. This is remarkable since the energies of reaction show an opposite preference. Thus the ancillary ligand X influences the energy barrier and the energy of reaction in opposite manners.

It was shown that the transition states **5** and **6** have geometrical features similar to that of the hydrido–ethylene complexes **1** and **3**: it is thus possible to discuss the energy barriers in term of the interaction energies of an ethylene moiety CH_2=CH_2 with a metal fragment RuL_2HX^{+q}.[2,3] The thermodynamic cycle of Fig. 2 show how the energy barrier, E_a, can be described by steps **a**, **b**, **c** and **d**. Step **a** corresponds to the dissociation of the reactant in a metal fragment and ethylene, keeping the geometries of the species identical to that in the reactant. The energy associated with step **a**, EI_R, which is the difference between the sum of the energies of the fragments and the energy of the reactant, differ from the previously calculated BDE where the geometries of the isolated fragments are optimized. Reverse of step **b** defines a transformation similar to step **a** for the transition state with the associated energy EI_{TS}. Since the energies are calculated in the direction of the arrows, the energy associated with step **a** is positive and that associated with step **b** negative. Steps **c** and **d** describe the deformation energies of the ethylene (Def_E) and metal fragment (Def_M) from

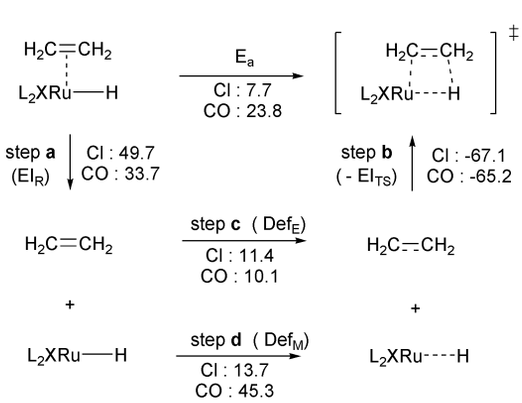

Fig. 2 Thermodynamic cycle for the analysis of the energy barrier for the insertion of ethylene in the Ru–H bond of species **1** and **3**, energies in kcal mol^{-1}. The structures for the top line are optimized, and for the two bottom lines are frozen in the geometries corresponding to the top line.

the geometries in the reactant to that in transition state. The values shown in Fig. 2 give the energies in the case of ethylene plus RuL_2HX^{+q} (X = Cl, q = 0; X = CO, q = 1).

We first discuss steps **a** and **b** in order to understand the variations in the interaction energies between CH_2=CH_2 and the metal fragment upon change of X. For X = Cl and CO, $|EI_{TS}|$ is larger than EI_R which is consistent with the shorter Ru–C_α and C_β–H in the TS than in the reactant. The variation in |EI| from ethylene complex to TS is larger for CO (EI_R = 33.7 kcal mol^{-1} in **3**, $|EI_{TS}|$ = 65.2 kcal mol^{-1} in **6**) than for Cl (EI_R = 49.7 kcal mol^{-1} in **1**, $|EI_{TS}|$ = 67.1 kcal mol^{-1} in **5**). The values of EI_{TS} are thus similar for Cl and CO. In contrast, the values for EI_R are significantly different for X = Cl and CO. If no other effects were involved, this would lead to an energy barrier lower for CO which is not the case. Deformation of ethylene (Def_E) in step **c** is similar for X = Cl and CO, but Def_M (step **d**) is more than 30 kcal mol^{-1} larger for CO (Def_M = 45.3 kcal mol^{-1}) than for Cl (Def_M = 13.7 kcal mol^{-1}). The deformations of CH_2=CH_2 and of the metal fragment along the reaction path from the ethylene adduct to the alkyl complex are both responsible for the activation barrier for the insertion reaction, but Def_M is specifically the origin of the difference in the barriers between Cl and CO. It costs more energy to distort $RuL_2(CO)H^+$ than RuL_2ClH from that the geometry in the reactant to that in the TS. The crucial geometrical change is the H–Ru–X angle. A simple molecular orbital analysis explains this behavior. The three doubly occupied d orbitals of d^6 ML_4 are shown in Scheme 2.

Two occupied d orbitals are stabilized by the π^*_{CO} orbitals in $RuL_2(CO)H^+$ and destabilized by the lone pairs of Cl in RuL_2-ClH. The d_π/p_π interactions are lost when the H–Ru–X angle increases from around 90° to its value (around 140°) in the TS. This is unfavorable for CO (Scheme 2) and favorable for Cl. Furthermore the orbital that X uses for making the Ru–X σ bond interacts with the occupied d orbital in the H–Ru–X plane which is more unfavorable for a strong σ donor like CO. This is highlighted by the elongation of the Ru–C(O) bond in the TS (2.097 Å) compared to that in the reactant (1.905 Å) and alkyl product (1.854 Å) (Fig. 1).

(2) RuL_2ClH (L = PH_3) with ethylene or fluoroethylene

The influence of a substituent on the olefin has been examined in the case of fluoroethylene. The insertion of CH_2=CHF into

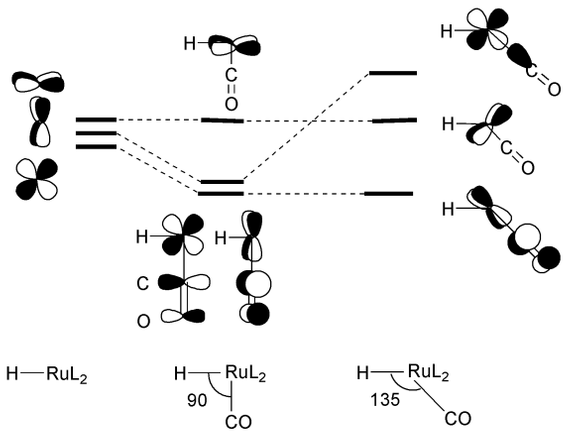

Scheme 2

the Ru–H bond of $Ru(PH_3)_2ClH$ leads to an alkyl complex with F on C_1 or C_2 (Fig. 3). This extends a study done on α-elimination with the same metal fragment.[17]

The structures of the fluoroethylene complexes (**7**) are similar to that of the ethylene complex **1** (Fig. 3). The presence of F leads to two isomers with F pointing toward (**7a**) or away from (**7b**) the vacant coordination site of Ru. These species are almost isoenergetic with **7a** only 1.1 kcal mol^{-1} more stable than **7b**, indicating no conformational preference for the fluoroethylene ligand. Similar lack of conformational preference have been obtained with CH_2=CH(OMe).[5] The presence of F shortens significantly the distance between Ru and the substituted carbon but has no consequence on the BDE of the olefin which remains similar for ethylene (39.2 kcal mol^{-1} in **1**) and fluoroethylene (39.1 kcal mol^{-1} in **7a**).

Insertion of fluoroethylene into Ru–H of **7a** gives an α-substituted alkyl complex **8a**. The insertion into Ru–H of **7b** gives the β-substituted alkyl complex **8b**. The alkyl complexes **8a** and **8b** are both stabilized by β C–H agostic interaction. The β C_2–H agostic is lengthened by presence of F on C_2 and shortened by F on C_1 compared to the reference structure **2**. The distance between Ru and the H of the agostic bond as well as the Ru–C_1–C_2 angle adjust accordingly (Fig. 3).

As for ethylene, the products of insertion of fluoroethylene are higher in energy than the reactants. The insertion reaction

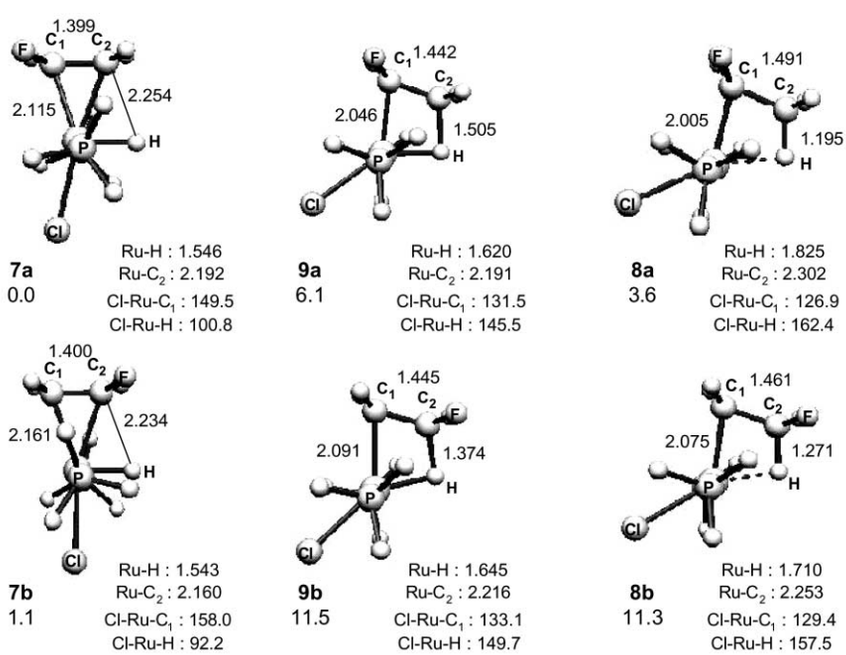

Fig. 3 Structures and relative energies of minima and transition states for the insertion of fluoroethylene in the Ru–H bond of $RuL_2(Cl)H$ for two different orientations: F on the α (C_1) carbon (top) and on the β (C_2) carbon (bottom). Distances are in Å, angles in °, energies in kcal mol^{-1}. The energy reference is **7a**.

with F on C_2 is endothermic by 10.2 kcal mol^{-1}, whereas it is only endothermic by 3.6 kcal mol^{-1} with F on C_1. Formation of the α-substituted alkyl complex is thus thermodynamically less disfavored. The energy pattern for the insertion of ethylene into the Ru–H bond (endothermic by 6.2 kcal mol^{-1}) is intermediate between the two substituted cases. These results are consistent with those found in the case of insertion of vinylether ligand [14] and are a reminder of the stabilizing influence of an heteroatom on a radical.[18] This shows that an heteroatomic group such as OMe or F favors the insertion of a substituted olefin for the formation of the α-substituted alkyl complex but not for the formation of the β-substituted alkyl complex.

The transition states from **7a(b)** to **8a(b)** are labeled **9a(b)**. The geometrical features of **5**, **9a** and **9b** are very similar as shown by the Ru–C_2 distances which differ by less than 0.03 Å and the C_1–C_2 distances which are equal within 0.003 Å. The major geometrical difference is found in the C_2–H distances (1.505 Å in **9a**, 1.473 Å in **5** and 1.375 Å in **9b**). These geometrical features follow the Hammond postulate since the geometry of the TS is closer to that of the alkyl complex as the reaction energy becomes more endothermic (6.1, 7.7 and 10.4 kcal mol^{-1}, respectively). The regioisomer with F on C_1 is thus preferred since it corresponds to a lower barrier and a less endothermic energy of reaction. In the case of **9b** the energy barrier is only 0.2 kcal mol^{-1} above **8b**. When the ZPE is added to the total energy for this later system, the TS is lower in energy than the product. This result shows that the harmonic approximation used to evaluate frequencies and ZPE is not valid in that case.

A thermodynamic cycle analogous to that used for ethylene (Fig. 4) has been used for the **7a** and **9a** and **7b** and **9b** transformations. The similar values found for steps **a**–**d** of the thermodynamic cycle are consistent with the similarity in the energy and geometry pattern discussed above. The interaction energies in **7a** and **7b** (EI_R) and also in **9a** and **9b** (EI_{TS}) differ by less than 0.3 kcal mol^{-1}. The slight differences in the distortion energies of the olefin and of the metal fragment are not significative.

In summary, substituting H by F in ethylene does not significantly alter the activation energies for the insertion of the olefin in the Ru–H bond (energy barrier varying by less than 6 kcal mol^{-1}) whereas the influence of the ancillary ligand X (Cl vs CO) at the metal center is considerably larger (energy barrier augmented by more than 15 kcal mol^{-1} from Cl to CO). Thus changing the olefin has much less consequence than changing a spectator ligand on the metal fragment. However, the orientation of the insertion as well as the nature of the spectator ligand on the metal have a notable influence on the energy of the alkyl complex. The alkyl complex is relatively stable for an α-substitution or X = CO and relatively less stable for a β-substitution or X = Cl.

(3) RuL_2ClH or RuL_2ClF (L = PH_3) with ethylene

In this section, we compare the insertion of ethylene into the Ru–H and the Ru–F bonds. We have studied the insertion of ethylene in the Ru–F bond for $RuL_2(Cl)(F)(CH_2{=}CH_2)$ and compared it to the insertion of ethylene in the Ru–H bond for $RuL_2(Cl)(H)(CH_2{=}CH_2)$. The reverse reaction (β-F abstraction) for the first system involves a C–F bond activation which is known to be a difficult reaction from experimental and theoretical studies.[19] This section extends the study of the insertion of carbene into the Ru–F and Ru–H bonds.[17]

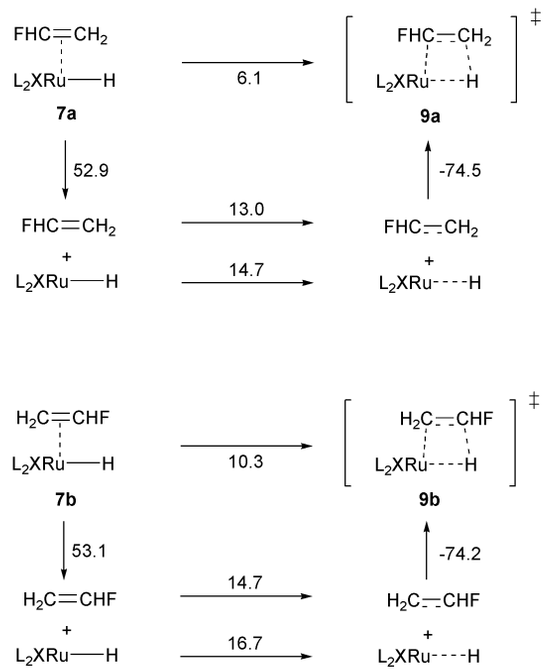

Fig. 4 Thermodynamic cycle for the analysis of the energy barrier for the insertion of fluoroethylene in the Ru–H bond of species **7**. The first (second) value corresponds to F going on C_1 (C_2) of the alkyl group. Energies are in kcal mol^{-1}. The structures for the top line are optimized, and for the two bottom lines are frozen in the geometries corresponding to the top line. Notations are similar to that in Fig. 2.

The olefin complex $RuL_2ClF(CH_2{=}CH_2)$ **10** is a square-based pyramid with ethylene coordinated at the apical site. The C–C axis of ethylene is perpendicular to the Ru–P axis, and eclipses the Ru–F bond (Fig. 5). This structure, which is found to be the most stable for the ethylene complex, is well adapted for the insertion of ethylene in the Ru–F bond. In contrast to the complexes previously discussed (**1** and **3**), the ethylene ligand in **10** is *trans* and not *cis* to the empty coordination site. The H–Ru–Cl angle in **1** is small (96.0°) and the F–Ru–Cl angle in **10** is large (149.7°), but both are far from 180° since the basal Cl and F ligands move away from the apical ethylene. Geometrical features for ethylene coordination to RuL_2FCl are indicative of a very strong ethylene–metal interaction. System **10** is closer to a metallacyclopropane than with the ethylene complexes discussed in this work. The Ru–C bonds are short (2.097 and 2.119 Å) and similar to a Ru–C single bond (close to that in an alkyl complex, 2.07 Å) and the C–C bond relatively long (1.423 Å). Despite these geometrical features, the BDE of ethylene to

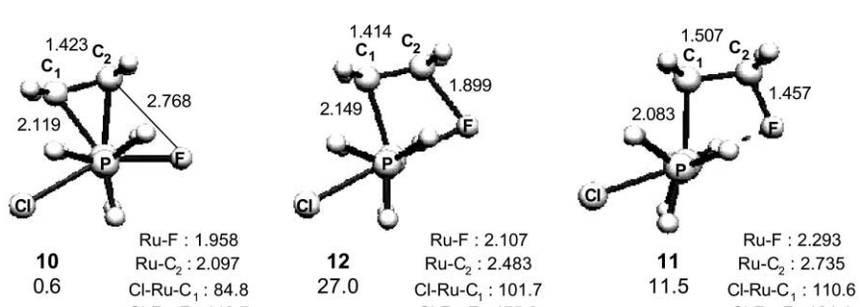

Fig. 5 Structures and relative energies of minima and transition states for the insertion of ethylene in the Ru–F bond of $RuL_2(Cl)F$. Distances are in Å, angles in °, energies in kcal mol^{-1}. The energy reference is **7a**.

RuL_2ClF, calculated between separated fragments in their singlet electronic state, is only 32.2 kcal mol^{-1}. This is smaller than the BDE of ethylene to RuL_2ClH (39.2 kcal mol^{-1}). It is thus not appropriate to associate univocally the strength of the BDE of ethylene to the metallacycle character of a complex, as already shown in several theoretical studies.[20]

The product of insertion of ethylene into the Ru–F bond is the β-substituted fluoroalkyl complex **11**. The β-substituent F interacts with the vacant coordination site (Ru ··· F distance of 2.293 Å). The alkyl complex **11** is 11.5 kcal mol^{-1} less stable than the ethylene complex **10**. Insertion of ethylene in the Ru–F bond in **10**, associated with formation of a C–F bond, is thus slightly more endothermic than insertion in the Ru–H bond in **1** (+6.2 kcal mol^{-1}) where a C–H bond is formed. Similar results from computational studies have been made for other reactions involving formation of C–F or C–H bonds.[17,21] This shows that the energy gained by the formation of the strong C–F bond in **11** is compensated by the cleavage of the strong Ru–F bond in **10**. Species **11** is a conformer of **9b** by rotation along the C_1–C_2 bond, in which a β C–H-agostic bond is replaced by the Ru ··· F interaction. These two species are quasi-isoenergetic (**11** is 0.2 kcal mol^{-1} above **8b**), which indicates that Ru ··· F and agostic interactions are energetically the same order of magnitude. Similar features were previously obtained in the case of an OMe substituent.[14]

The transition state for insertion of ethylene into the Ru–F bond, **12**, was found to have geometrical features similar to that of **5** (Fig. 5). The two TS can thus be described as distorted ethylene complexes. The Ru–F bond is short (2.107 Å in **12** *vs.* 1.958 Å in the olefin complex **10**) and the C–F distance is long (1.899 Å in **12** *vs.* 1.457 Å in the alkyl complex **11**). The C ··· C distance in the transition state **12** (1.414 Å) is even shorter than in the ethylene complex **10** (1.423 Å). The Ru ··· C_2 distance exhibits a greater difference between **12** and **5**: it considerably increases along the reaction path for insertion in the Ru–F bond (2.097 Å in **10**, 2.483 Å in **12** and 2.735 Å in **11**). In the case of insertion in the Ru–H bond, the Ru–C_β is almost identical in the olefin complex **1** (2.203 Å) and in the TS **5** (2.215 Å). The energy barrier is much higher for inserting into the Ru–F than in Ru–H bonds: the transition state **12** is 27.9 kcal mol^{-1} above the ethylene complex **10** compared to TS **5** which is only 7.7 kcal mol^{-1} above **1**. Insertion of ethylene into the Ru–F bond is thus kinetically strongly disfavored over insertion in the Ru–H bond in analogous systems.

A thermodynamic cycle analogous to those done previously was used to characterize the energy features for the **10** to **12** transformation (Fig. 6). The absolute value of interaction energy, $|EI_{TS}|$, between CH_2=CH_2 and the metal fragment in the transition state **12** is very small compared to the corresponding quantity EI_R in **10**. This is opposite to that obtained for insertion in the Ru–H bond : $|EI_{TS}|$ in **5** is larger than in **1**. The weak bonding interaction between the two fragments in **12** results in a high energy for this transition state structure. This weak bonding can be understood by comparing the HOMO in **5** and **12**

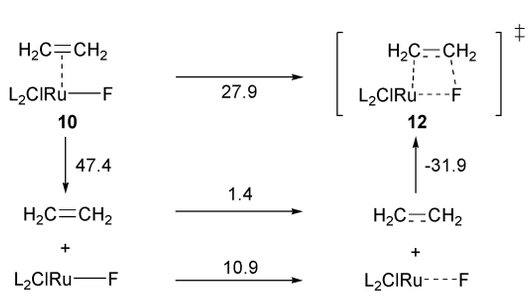

Fig. 6 Thermodynamic cycle for the analysis of the energy barrier for the insertion of ethylene in the Ru–F bond of species **10**. Energies are in kcal mol^{-1}. The structures for the top line are optimized, and for the two bottom lines are frozen in the geometries corresponding to the top line. Notations are similar to Fig. 2.

(Fig. 7). In TS **5**, the HOMO is mainly a d metal orbital, with a small bonding interaction with the β carbon. This favors a short Ru ··· C_β distance. In **12**, the HOMO has a similar nature to that in **5** but also exhibits an antibonding interaction with one lone pair on F (Fig. 7, top-right). This disfavors the formation of the C–F bond and is thus responsible for the long Ru ··· C_2 distance. Insertion of the carbene CH_2 into a Ru–F bond was also shown to have a high activation barrier because of the destabilizing role played by one lone pair of F.[17]

Species **9b** and **11** are conformers. Therefore the competition between H and F abstraction in the β-substituted alkyl complex $RuL_2Cl(CH_2CH_2F)$ can be discussed using the above results. The two alkyl complexes **9b** and **11** are isoenergetic. The product from β-F abstraction in **11** is the ethylene complex **10** which is only 1.7 kcal mol^{-1} above **7b**. Species **7b** is also the product from β-H abstraction in **9b**. There is no thermodynamic preference for either β-H or β-F abstraction. However, the β-F abstraction (**11** to **10**) requires a high energy barrier (16.4 kcal mol^{-1}) and the β-H abstraction (**9b** to **7b**) occurs with essentially no activation barrier (less than 0.5 kcal mol^{-1} energy barrier). The β-H abstraction is thus strongly kinetically favored over β-F abstraction.

This study shows that key features which were already noted in the case of C–H/C–F oxidative addition[21] and in α-H/α-F abstraction[17] (Scheme 3) are also found in the case of β-H/β-F abstraction. These three processes have similar features : C–F and C–H activation are thermodynamically competitive (C–F activation is systematically slightly favored in these three cases) but C–F activation has always a high energy barrier. Activation of C–F or C–H to form metal–F or metal–H bonds, respectively, may be thermodynamically competitive, and not systematically in favor of metal–H bond formation. This may be a general result as proposed in recent studies of BDE in L_nMX.[22] It is more difficult to generalize the results on the energy barriers since this present study has shown that they are greatly dependent on the coordination of the metal center. However, from this present study as well as from published results,[17] it appears that the high barrier for cleaving C–F bond is related to the presence of a repulsive interaction between the metal d electrons and the F lone pairs. This suggests that d^0 metal center may react with C–F bond with considerably lower barriers. This has been shown by DFT calculations to be the case for some Zr(IV) complexes.[23] Furthermore C–F bond activation by d^0 metal center is well documented.[24]

Conclusions

DFT computations have been carried out to study the activation barriers and transition state structures for the insertion of an olefin in the Ru–H or Ru–F bond of unsaturated 16-electron pentacoordinated complexes $RuL_2XH(olefin)^{+q}$ (X = Cl, q = 0; X = CO, q = 1) or $RuL_2ClF(CH_2$=$CH_2)$, to give 14-electron tetracoordinated β-agostic alkyl complexes. Low activation barriers have been found in the case of insertion of ethylene or fluoroethylene in the Ru–H bound of the metal fragment RuL_2HCl. Using the olefin complexes as energy references, substitution of an H by an F on ethylene stabilizes the alkyl complex only if F is at the α position; a destabilisation is observed if F is on the β position of the alkyl group. The energy barriers for insertion follow the relative energies of the alkyl products: the energy barrier is the lowest for insertion of fluoroethylene with F going to the α carbon of the alkyl chain, the energy barrier is the highest for insertion of fluoroethylene with F going on the β carbon and the energy barrier in the case of ethylene is intermediate. These features follow the Hammond postulate. In contrast, high energy barriers and unusual geometrical features with non-monotonic variation of bond lengths along the reaction path have been found with a π-acceptor ligand (CO) on Ru. The energy barrier for insertion of ethylene in the Ru–H bond is over 15 kcal mol^{-1} higher for $RuL_2H(CO)(CH_2$=$CH_2)^+$ than for

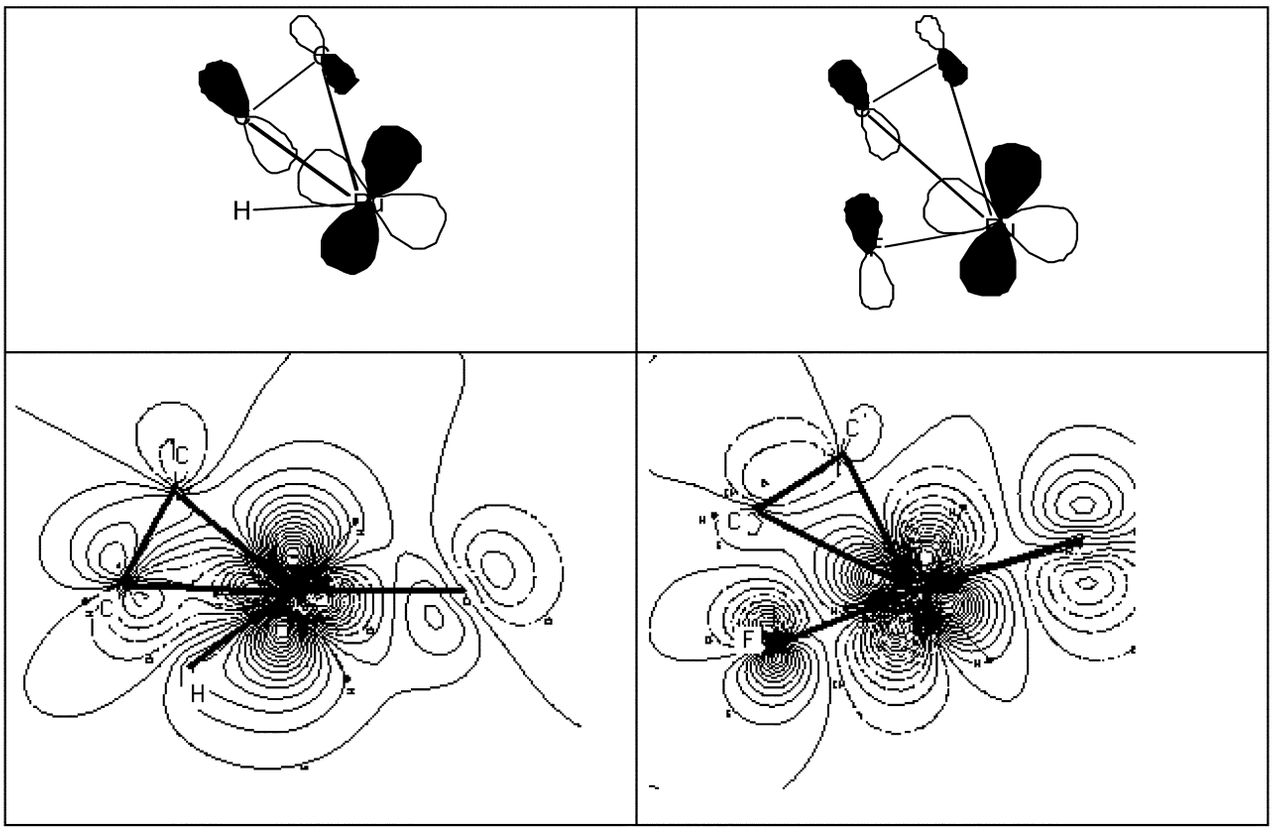

Fig. 7 HOMO for **5** (left) and **12** (right): schematic representation (top) and isocontours in the Y–Ru–C_2 plane (bottom) (Y = H, F).

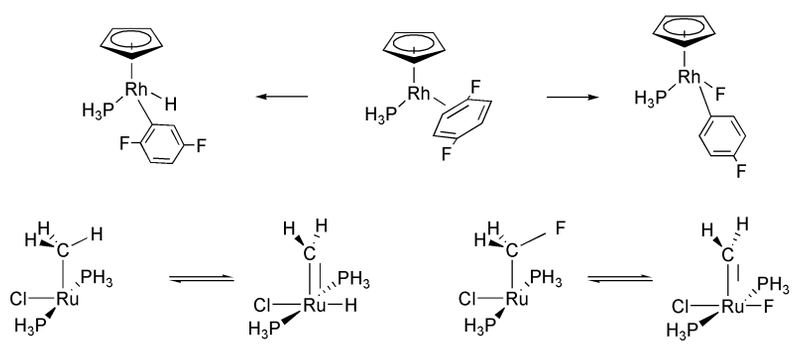

Scheme 3

$RuL_2H(Cl)(CH_2{=}CH_2)$. The energy barrier for the insertion in the Ru–F bond of $RuL_2F(Cl)(CH_2{=}CH_2)$ has also a very high barrier. This later result generalizes the results found on the high barriers associated with C–F α-migration,[16] C–F oxidative addition,[21] and migration in the proximity of F.[25] Using an energy decomposition based on a thermodynamic cycle, it is shown that the high energy barrier for insertion of ethylene in the Ru–H bond of $RuL_2H(CO)(CH_2{=}CH_2)^+$ is due to the rigidity of the metal fragment $RuL_2H(CO)^+$ which energetically disfavors the change of coordination necessary to go from reactant to product. In the case of insertion ethylene in the Ru–F bond, the high activation barrier is associated with the presence of an F lone pair coplanar with the ethylene ligand which creates some destabilizing interaction with the π orbital of ethylene.

Acknowledgements

This study was inspired from the experimental studies obtained in the group of Professor K. G. Caulton (Indiana University). The authors are grateful to Professor E. R. Davidson (Indiana University) for initiating the study and for insightful discussions and Indiana University computing center for generous donation of computational time. They thank Dr E. Clot (Université Montpellier) for useful contributions.

References

1 R. H. Crabtree, *The Organometallic Chemistry of the transition Metals*, Wiley, New York, NY, 3rd edn., 2000.
2 S. Niu and M. B. Hall, *Chem. Rev.*, 2000, **100**, 353.
3 N. Koga and K. Morokuma, *Transition Metal Hydrides*, ed. A. Dedieu, VCH, New York, 1992, p. 185.
4 M. Oliván, E. Clot, O. Eisenstein and K. G. Caulton, *Organometallics*, 1998, **17**, 3091.
5 J. N. Coalter III, J. C. Bollinger, J. C. Huffman, U. Werner-Zwanziger, K. G. Caulton, E. R. Davidson, H. Gérard, E. Clot and O. Eisenstein, *New J. Chem.*, 2000, **24**, 9.
6 D. Huang, J. C. Bollinger, W. E. Streib, K. Folting, V. Young Jr., O. Eisenstein and K. G. Caulton, *Organometallics*, 2000, **19**, 2281.
7 A. D. Becke, *J. Chem. Phys.*, 1993, **98**, 5648.
8 J. P. Perdew and Y. Wang, *Phys. Rev., B*, 1992, **45**, 13244.
9 M. J. Frisch, G. W. Trucks, H. B. Schlegel, G. E. Scuseria, M. A. Robb, J. R. Cheeseman, V. G. Zakrzewski, J. A. Montgomery Jr., R. E. Stratmann, J. C. Burant, S. Daprich, J. M. Millam, A. D. Daniels, K. N. Kudin, M. C. Strain, O. Farkas, J. Tomasi, V. Barone, M. Cossi, R. Cammi, B. Mennucci, C. Pomelli, C. Adamo, S. Clifford, J. Ochterski, G. A. Petersson, P. Y. Ayala, Q.

Cui, K. Morokuma, D. K. Malick, A. D. Rabuck, K. Raghavachari, J. B. Foresman, J. Cioslowski, J. V. Ortiz, A. G. Baboul, B. B. Stefanov, G. Liu, A. Liashenko, P. Piskorz, I. Komaromi, R. Gomperts, R. L. Martin, D. J. Fox, T. Keith, M. A. Al-Laham, C. Y. Peng, A. Nanayakkara, C. Gonzalez, M. Challacombe, P. M. W. Gill, B. Johnson, W. Chen, M. W. Wong, J. L. Andres, M. Gonzalez, M. Head-Gordon, E. S. Replogle and J. A. Pople, Gaussian 98, Revision A.7, Gaussian, Inc., Pittsburgh, PA, 1998.
10 P. G. Hay and W. R. Wadt, *J. Chem. Phys.*, 1985, **82**, 299.
11 W. R. Wadt and P. G. Hay, *J. Chem. Phys.*, 1985, **82**, 184.
12 A. H. Höllwarth, M. B. Böhme, S. Dapprich, A. W. Ehlers, A. Gobbi, V. Jonas, K. F. Köhler, R. Stegman, A. Veldkamp and G. Frenking, *Chem. Phys. Lett.*, 1993, **208**, 237.
13 P. C. Hariharan and J. A. Pople, *Theor. Chem. Acta*, 1973, **28**, 213.
14 H. Gérard, E. Clot, C. Giessner-Prettre, K. G. Caulton, E. R. Davidson and O. Eisenstein, *Organometallics*, 2000, **19**, 2291.
15 M. L. H. Green and M. Brookhart, *J. Organomet. Chem.*, 1983, **250**, 395; M. Brookhart, M. L. H. Green and L. L. Wong, *Prog. Inorg. Chem.*, 1986, **36**, 1; R. H. Crabtree and D. G. Hamilton, *Adv. Organomet. Chem.*, 1989, **28**, 299.
16 J. March, *Advanced Organic Chemistry*, John Wiley & Sons, New York, 4th edn., 1992.
17 H. Gérard, E. R. Davidson and O. Eisenstein, *Mol. Phys.*, 2002, **100**, 533; G. Ferrando-Miguel, H. Gérard, O. Eisenstein and K. G. Caulton, *Inorg. Chem.*, 2002, **41**, 6440.
18 G. Leroy, *Adv. Quantum Chem.*, 1985, **17**, 1; W. J. Hehre, L. Radom, P. v. R. Schleyer and J. A. Pople, *Ab Initio Molecular Orbital Theory*, Wiley, New York, 1986, p. 348; P. M. Mayer, N. Glukhopvstev, J. W. Gauld and L. Radom, *J. Am. Chem. Soc.*, 1997, **119**, 12889; J. W. Gauld, J. L. Holmes and L. Radom, *Acta Chem. Scand.*, 1997, **51**, 641.
19 (*a*) R. P. Hughes, *Adv. Organomet. Chem.*, 1990, **31**, 183; (*b*) J. L. Kipplinger, T. G. Richmond and C. E. Osterberg, *Chem. Rev.*, 1994, **94**, 373; (*c*) T. G. Richmond, *Angew. Chem. Int. Ed.*, 2000, **39**, 3241; (*d*) T. G. Richmond, in *Topics in Organometallic Chemistry, Activation of Unreactive Bonds and Organic Synthesis*, ed. S. Murai,, Springer-Verlag1999, New York, p. 244; (*e*) M. Aizenberg and D. Milstein, *Science*, 1994, **265**, 359; (*f*) T. Braun, S. P. Foxon, R. N. Perutz and P. H. Walton, *Angew. Chem., Int. Ed.*, 1999, **38**, 3326; (*g*) T. Braun, D. Noveski, B. Neumann and H.-G Stammler, *Angew. Chem., Int. Ed.*, 2002, **41**, 2745.
20 G. Frenking and N. Fröhlich, *Chem. Rev.*, 2000, **2**, 717, and references therein.
21 R. Bosque, S. Fantacci, E. Clot, F. Maseras, O. Eisenstein, R. N. Perutz, K. B. Renkema and K. G. Caulton, *J. Am. Chem. Soc.*, 1998, **120**, 12634, and references therein.
22 (*a*) W. D. Jones and E. T. Hessel, *J. Am. Chem. Soc.*, 1993, **115**, 554; (*b*) D. D. Wick and W. D. Jones, *Organometallics*, 1999, **18**, 495; (*c*) H. E. Bryndza, L. K. Fong, R. A. Paciello, W. Tam and J. E. Bercaw, *J. Am. Chem. Soc.*, 1987, **109**, 1444; (*d*) P. L. Holland, R. A. Andersen, R. G. Bergman, J. Huang and S. P. Nolan, *J. Am. Chem. Soc.*, 1997, **119**, 12800; (*e*) E. Clot, M. Besora, F. Maseras, O. Eisenstein, B. Oelckers and R. N. Perutz, *Chem. Commun.*, 2003, DOI: 10.1039/b210036n.
23 L. A. Watson, D. V. Yandulov and K. G. Caulton, *J. Am. Chem. Soc.*, 2001, **123**, 603.
24 B. M. Kraft and W. D. Jones, *J. Am. Chem. Soc.*, 2002, **124**, 8681, and references therein.
25 J. J. Carbó, O. Eisenstein, C. L. Higgit, A. Hugo Klahn, F. Maseras, B. Oelckers and R. N. Perutz, *J. Chem. Soc., Dalton Trans.*, 2001, 1452.